25th ABCM International Congress of Mechanical Engineering
October 20-25, 2019, Uberlândia, MG, Brazil

COB-2019-0712
COMPARISON BETWEEN TWO AND THREE-DIMENSIONAL DIRECT NUMERICAL SIMULATIONS OF ROSSITER MODES IN OPEN CAVITY FLOW

Marlon Sproesser Mathias
Marcello A. F. Medeiros
São Carlos School of Engineering - University of São Paulo
marlon.mathias@usp.br
marcello@sc.usp.br

Abstract. *We simulate a compressible flow in an open cavity using our Direct Numerical Simulation code (DNS) in both two and three-dimensional setups. Our goal is to measure the effects of three-dimensional phenomena, such as centrifugal instabilities, over the essentially two-dimensional Rossiter modes. An open cavity flow is set up so that both types of modes are present. The flow is simulated until it's well developed. When three-dimensional effects are included, a different Rossiter mode becomes the dominant in the flow. Centrifugal modes can also be observed by looking at the temporal spectrum, which matches our linear predictions. The goal is to understand the limitations and applicability of the much cheaper two-dimensional simulations both on linear and non-linear analysis.*

Keywords: *Direct numerical simulation, Rossiter modes, Centrifugal instability, Open cavity flow*

1. INTRODUCTION

Open rectangular cavities are simple geometries that can be used to represent various kinds of more complex flows. A better understanding of flow instability phenomena in this simplified case may help improving the aerodynamic design of various devices. The flow and its parameters are illustrated in Fig. 1. Two and three dimensional instabilities may occur depending on certain flow parameters.

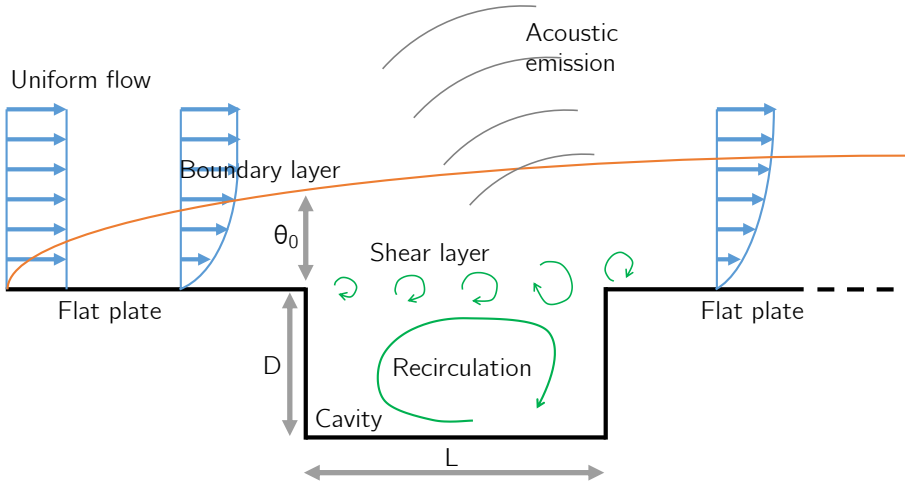

Figure 1. Schematics of an open cavity flow.

In previous studies, two-dimensional simulations and BiGlobal instability analysis were used to better understand the mechanism Rossiter modes become unstable in the cavity (Rossiter, 1964; Mathias and Medeiros, 2018b; Yamouni *et al.*, 2013). These modes are two-dimensional and non-linear, therefore this linear approximation is valid only for the initial phases. Sipp and Lebedev (2007) show that this linear approximation is also valid under certain conditions, especially if the flow is not far from its critical instability conditions.

Some other studies have analyzed the three-dimensional flow instability by setting a fixed span-wise wave number (de Vicente *et al.*, 2014). These are the so-called centrifugal modes, or Görtler vortices modes.

Our goal is to set up a case where both these instabilities may occur at the same time so the influence of the three-dimensional modes over the two-dimensional ones can be observed.

2. METHODS

2.1 Numerical methods

An in-house Direct Numerical Solver for the compressible Navier-Stokes equation (DNS) was used (Martinez and Medeiros, 2016). Global instability modes of the flow may also be retrieved using a time-stepping approach that runs on top of this DNS (Mathias and Medeiros, 2018a).

The computational mesh is structured and can be stretched in regions of interest. A fourth order Runge-Kutta scheme is used for time marching and fourth order compact spectral-like finite differences are used for the spatial derivatives (Lele, 1992). A tenth-order spatial high-frequency filter is also employed to avoid problems with aliasing (Gaitonde and Visbal, 1998).

Buffer zones are placed around the domain to attenuate undesirable boundary condition effects such as reflections. They employ a combination of grid stretching, lower order spatial derivatives and Selective Frequency Damping (SFD) (Åkervik *et al.*, 2006). The SFD acts as a low pass temporal filter and may also be turned on in the whole domain to allow base flows to be generated faster or at unstable conditions.

The code is capable of simulating both two and three-dimensional flows over any Cartesian geometry and uses a pencil-slab domain decomposition for computational parallelization (Li and Laizet, 2010).

2.2 Flow parameters

The simulation was set to $Re_D = 1000$, based on the cavity depth; the cavity aspect ratio is $L/D = 2$; the incoming boundary layer momentum thickness is $D/\theta = 100$; and the Mach number is $Ma = 0.5$. We have selected those parameters as previous two dimensional simulations have pointed it to be considerably unstable (Mathias and Medeiros, 2018b).

Our intention was to set up a case where both two and three dimensional instabilities appear, therefore a high D/θ ratio was selected. It tends to make three dimensional centrifugal modes more unstable due to the increased recirculation strength in the cavity (Brès and Colonius, 2008). A thin boundary layer also aids two dimensional instabilities due to the thin mixing layer over the cavity.

For the span-wise domain length definition, the global instability algorithm was used and pointed that the most unstable centrifugal mode happens around a span-wise wave number of $\beta = 2\pi$, which translates into a span-wise length equal to the cavity depth.

2.3 Simulation parameters

The mesh used in this study is $300 \times 200 \times 64$ in the stream-wise, wall-normal and span-wise directions respectively. 20 extra nodes are added as buffer zones in each of the open boundary conditions, totaling $340 \times 220 \times 64$ nodes. The mesh is refined close to the cavity opening in both flow and wall-normal directions. In the stability analysis, the span-wise mesh was reduced to 8 nodes.

The origin is set to the leading edge of the flat plate and all lengths are in terms of cavity depths. The domain covers $-1 \leq X \leq 5$ in the stream-wise direction. Before the flat plane, a free-slip region is used for the flow pressure to settle after the boundary conditions. The wall-normal direction spans $-1 \leq Y \leq 4$. And the span-wise direction is periodic and covers $0 \leq Z \leq 1$.

The cavity leading edge is at $X = 0.227$ so that the desired incoming boundary layer thickness is achieved.

The initial flow for the simulation was obtained by running the DNS with a strong temporal low-pass filter on the whole domain so that all instabilities are damped out. A small span-wise disturbance was added afterwards to aid triggering three-dimensional instabilities.

3. RESULTS

3.1 Global instability results

We used the global instability analysis for two reasons. First, the span-wise length of the simulation domain should be such that centrifugal instability would happen. Second, it would indicate the expected frequencies of both two and three dimensional instabilities as well as their growth rates, at least for the linear phase.

The results of the span-wise wave number sweep are shown in Fig. 2. Each eigenvalue in the complex plane relates to an instability mode. A positive real part (x-axis) indicates an unstable mode. The imaginary part (y-axis) relates to the temporal frequency.

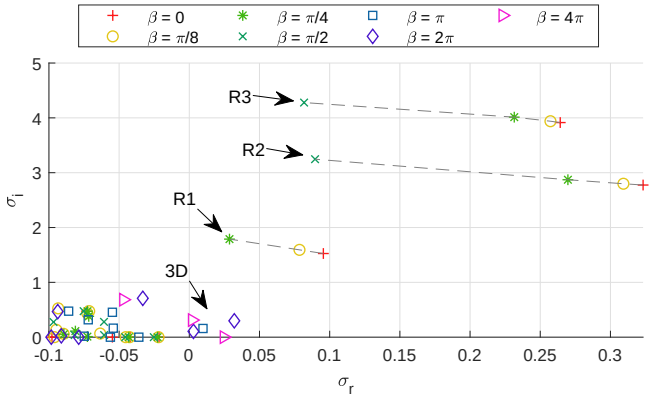

Figure 2. Eigenvalues from the global stability analysis. A positive real part (x-axis) indicates an unstable mode. The imaginary part (y-axis) relates to the temporal frequency. Rossiter modes 1 to 3 are indicated as R_N and the centrifugal modes are indicated as 3D.

The span-wise wave number with the most unstable 3D mode was $\beta = 2\pi$, with an wavelength of 1, therefore, that is the domain periodicity in the span-wise direction that should be used in the simulations. Note that any multiple of 1 should also work, but the computational cost would be considerably increased.

Rossiter modes were also visible in the 3D analysis with the largest span-wise domains (i.e. the lowest wave numbers), which were already approaching the 2D case.

3.2 Simulation results

Figure 3 shows density isosurfaces of a snapshot of the 3D flow after the initial transient has dissipated. Visually, the dominant mode in the cavity seems to be 2D, with a slight modulation in the span-wise direction.

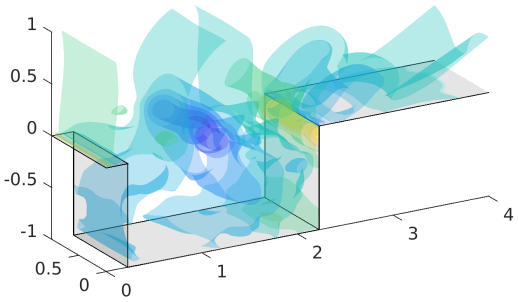

Figure 3. Snapshot of the flow at an arbitrary time, after the initial transient. Surfaces indicate constant density.

We used the temporal signal from a probe midway through the cavity opening to get the flow spectrum, so it could be compared to the linear predictions and to the two-dimensional results. Figure 4 shows the temporal data and its resulting spectrum from the streamwise velocity for both 2D and 3D cases. The spectrum through time was obtained with the use of Hanning windows.

Figure 5 shows the spectra after the initial transient is dissipated for both 2D and 3D cases. There is a clear shift from Rossiter mode 1 to mode 2 when 3D effects are also accounted for. This happens despite the fact that the 3D centrifugal mode is much weaker than the 2D modes both in the spectrum and in the linear stability analysis.

The three dimensional case is also considerably mode chaotic, with a visible broadband signal in the spectrum. The frequencies in the 3D case have also increased slightly when compared to the 2D simulation. The Rossiter 2 peak has shifted from $\omega = 2.68$ to $\omega = 2.75$.

3.3 Influence of the mean flow

As seen in the previous section, despite being considerably less unstable and less present in the spectrum, the 3D effects do play an important role in selecting the dominant Rossiter mode.

We have computed the mean flow for both 2D and 3D cases by averaging several snapshots of the flows after the initial transient has dissipated. Figure 6 depicts the change in the mixing layer thickness over the cavity. The thickness af each

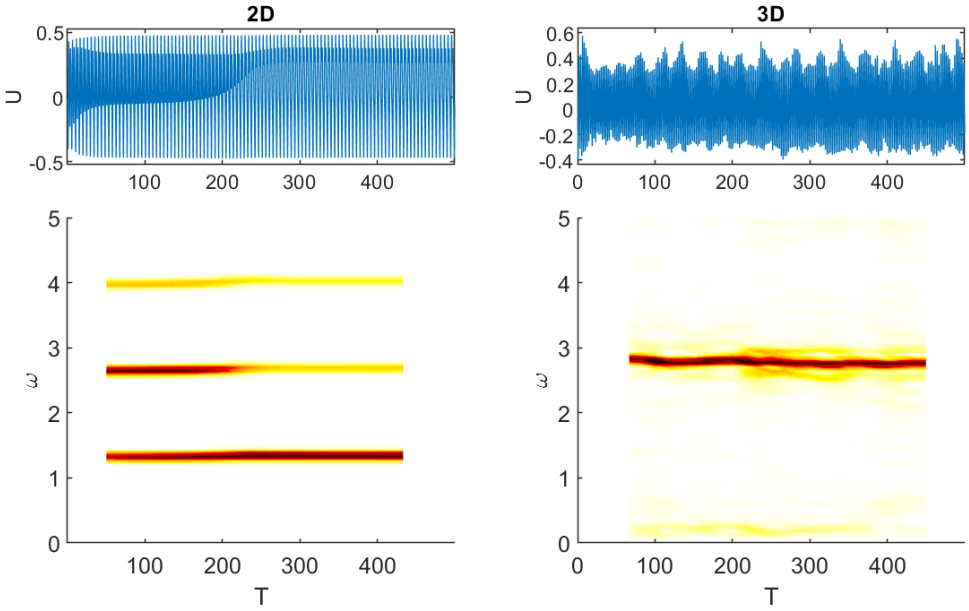

Figure 4. Stream-wise velocity at the cavity opening midpoint (top) and spectra through time (bottom) for 2D and 3D simulations.

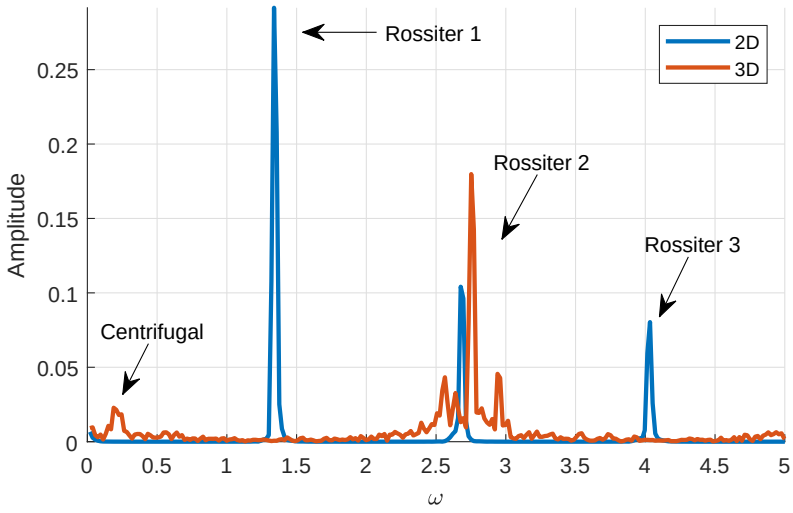

Figure 5. Spectra after the initial transient for 2D and 3D simulations.

point is measured as $T = U_\infty / \max(\partial U / \partial y)$.

Both mean flows considerably increased the mixing layer thickness. When the three-dimensional effects are included, this increase was lower and more uniform across the cavity. This can be attributed to the fact that span-wise fluid motion may cause flow structures to dissipate more easily into the smaller scales.

The thinner mixing layer in the 3D simulation explains the slightly higher frequencies in this case, as the vortices travel faster across the cavity opening.

Figure 7 shows that while both mean flows have an increased backwards flow inside the cavity, in the 2D case, this effect is stronger and peaks closer to the mixing layer.

The global stability analysis routine was used on both mean flows so we could determine how much this new mixing layer and backwards flow would affect the linear stability. In both cases, the thicker mixing layer of the mean flows reduce the linear growth rates of the Rossiter modes. Mode 1 becomes slightly stable for both cases. Mode 2 remains unstable, but its growth rate is considerably larger in the 3D case, which might explain why the second mode is much more present in the 3D simulation, along with the fact that 2D scenarios favor larger structures, such as the ones present in the first Rossiter mode.

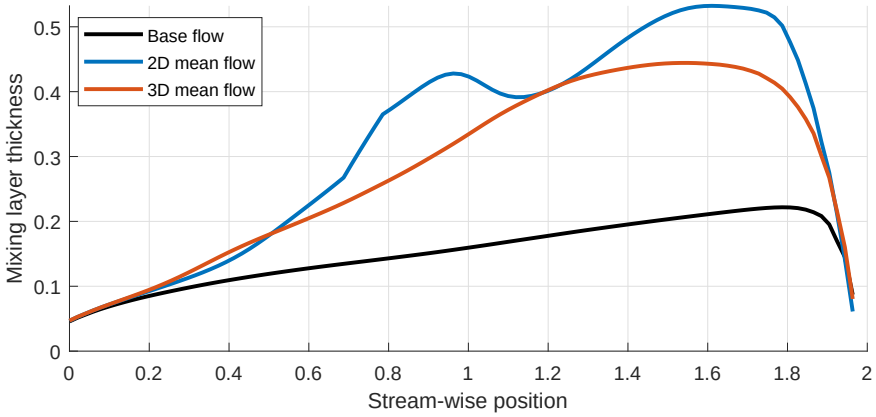

Figure 6. Mixing layer thickness across the cavity for the base flow, and both mean flows.

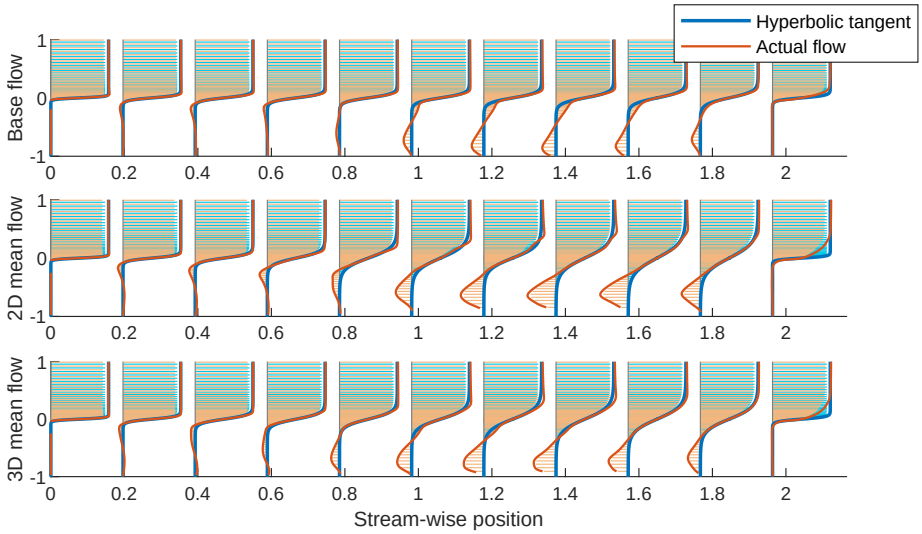

Figure 7. Mixing layer profiles across the cavity for the base flow, and both mean flows.

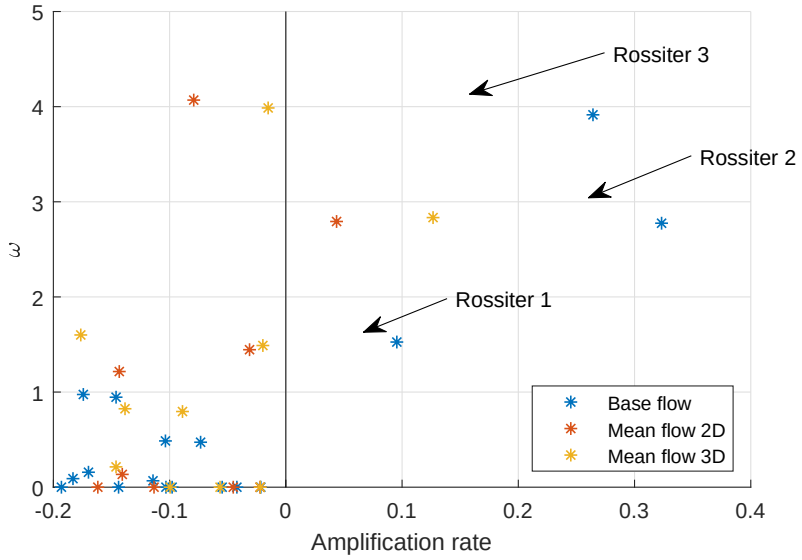

Figure 8. .

4. DISCUSSION

An open cavity case that was deemed critical for both two and three dimensional instabilities, due to a thin incoming boundary layer, was simulated in our DNS until both types of instabilities were present. The results show that the three

dimensional effects, such as centrifugal instabilities, may cause the flow to favor a different Rossiter mode than in a two dimensional scenario.

This change may be partially explained by the difference in the mean flow in both cases. The 3D case has a mean flow with a slightly thinner mixing layer, which grows in a smoother fashion.

An important outcome of this result is that two-dimensional simulations are still valid particularly at the linear phases of the instability growth. At more non-linear situations, especially if turbulence is expected to be present, a full three-dimensional simulation may be needed, even if the most apparent modes are two-dimensional.

5. ACKNOWLEDGMENTS

The authors would like to thank the São Paulo Research Foundation (FAPESP/Brazil), for grants 2018/04584-0 and 2017/23622-8; the National Council for Scientific and Technological Development (CNPq/Brazil) for grants 134722/2016-7 and 304859/2016-8; the US Air Force Office of Scientific Research (AFOSR) for grant FA9550-18-1-0112, managed by Dr. Geoff Andersen from SOARD; and Professor Vasilios Theofilis of the University of Liverpool for the support during the project and for providing access to the Barkla cluster.

6. REFERENCES

Åkervik, E., Brandt, L., Henningson, D.S., Hœpffner, J., Marxen, O. and Schlatter, P., 2006. "Steady solutions of the Navier-Stokes equations by selective frequency damping". *Physics of Fluids*, Vol. 18, No. 6, p. 068102. ISSN 10706631. doi:10.1063/1.2211705. URL http://scitation.aip.org/content/aip/journal/pof2/18/6/10.1063/1.2211705.

Brès, G.A. and Colonius, T., 2008. "Three-dimensional instabilities in compressible flow over open cavities". *Journal of Fluid Mechanics*, Vol. 599, pp. 309–339. ISSN 0022-1120. doi:10.1017/S0022112007009925. URL http://www.journals.cambridge.org/abstract_S0022112007009925.

de Vicente, J., Basley, J., Meseguer-Garrido, F., Soria, J. and Theofilis, V., 2014. "Three-dimensional instabilities over a rectangular open cavity: from linear stability analysis to experimentation". *Journal of Fluid Mechanics*, Vol. 748, pp. 189–220. ISSN 0022-1120. doi:10.1017/jfm.2014.126. URL http://www.journals.cambridge.org/abstract_S0022112014001268.

Gaitonde, D.V. and Visbal, M.R., 1998. "High-Order Schemes for Navier-Stokes Equations: Algorithm and Implementation Into FDL3DI". Technical report, Wright-Patterson Air Force Base.

Lele, S.K., 1992. "Compact finite difference schemes with spectral-like resolution". *Journal of Computational Physics*, Vol. 103, No. 1, pp. 16–42. ISSN 00219991. doi:10.1016/0021-9991(92)90324-R.

Li, N. and Laizet, S., 2010. "2DECOMP & FFT-A Highly Scalable 2D Decomposition Library and FFT Interface". *Cray User Group 2010 conference*, pp. 1–13.

Martinez, A. and Medeiros, M.F., 2016. "Direct numerical simulation of a wavepacket in a boundary layer at Mach 0.9". In *46th AIAA Fluid Dynamics Conference*. American Institute of Aeronautics and Astronautics, Reston, Virginia, Vol. 414, pp. 1–33. ISBN 978-1-62410-436-7. ISSN 00221120. doi:10.2514/6.2016-3195. URL http://arc.aiaa.org/doi/10.2514/6.2016-3195.

Mathias, M.S. and Medeiros, M., 2018a. "Direct Numerical Simulation of a Compressible Flow and Matrix-Free Analysis of its Instabilities over an Open Cavity". *Journal of Aerospace Technology and Management*, Vol. 10, pp. 1–13. ISSN 2175-9146. doi:10.5028/jatm.v10.949. URL http://www.jatm.com.br/ojs/index.php/jatm/article/view/949.

Mathias, M.S. and Medeiros, M.F., 2018b. "The Influence of the Boundary Layer Thickness on the Stability of the Rossiter Modes of a Compressible Rectangular Cavity". In *2018 Fluid Dynamics Conference*. American Institute of Aeronautics and Astronautics, Reston, Virginia. ISBN 978-1-62410-553-1. doi:10.2514/6.2018-3386. URL https://arc.aiaa.org/doi/10.2514/6.2018-3386.

Rossiter, J.E., 1964. "Wind-tunnel experiments on the flow over rectangular cavities at subsonic and transonic speeds". Technical Report Aeronautical Research Council Reports and Memoranda 3438, Ministry of Aviation, London. URL http://repository.tudelft.nl/view/aereports/uuid:a38f3704-18d9-4ac8-a204-14ae03d84d8c/.

Sipp, D. and Lebedev, A., 2007. "Global stability of base and mean flows: a general approach and its applications to cylinder and open cavity flows". *Journal of Fluid Mechanics*, Vol. 593. ISSN 0022-1120. doi:10.1017/S0022112007008907.

Yamouni, S., Sipp, D. and Jacquin, L., 2013. "Interaction between feedback aeroacoustic and acoustic resonance mechanisms in a cavity flow: a global stability analysis". *Journal of Fluid Mechanics*, Vol. 717, pp. 134–165. ISSN 0022-1120. doi:10.1017/jfm.2012.563. URL http://www.journals.cambridge.org/abstract_S0022112012005630.

7. RESPONSIBILITY NOTICE

The following text, properly adapted to the number of authors, must be included in the last section of the paper: The authors are the only responsible for the printed material included in this paper.